J Cachexia Sarcopenia Muscle
DOI 10.1007/s13539-012-0071-9

ORIGINAL ARTICLE

Cancer cachexia is associated with a decrease in skeletal muscle mitochondrial oxidative capacities without alteration of ATP production efficiency

Cloé M. Julienne · Jean-François Dumas · Caroline Goupille · Michelle Pinault · Cécile Berri · Anne Collin · Sophie Tesseraud · Charles Couet · Stephane Servais

Received: 25 August 2011 / Accepted: 30 April 2012

Abstract
Background Cancer cachexia is a complex syndrome related to a negative energy balance resulting in muscle wasting. Implication of muscle mitochondrial bioenergetics alterations during cancer cachexia was suggested. Therefore, the aim of this study was to explore the efficiency of oxidative phosphorylation in skeletal muscle mitochondria in a preclinical model of cancer cachexia.
Methods Berlin–Druckrey IX rats with peritoneal carcinosis (PC) were used as a model of cancer cachexia with healthy pair-fed rats (PF) as control. Hindlimb muscle morphology and fibre type composition were analysed in parallel with ubiquitin ligases and UCP gene expression. Oxidative phosphorylation was investigated in isolated muscle mitochondria by measuring oxygen consumption and ATP synthesis rate.
Results PC rats underwent significant muscle wasting affecting fast glycolytic muscles due to a reduction in fibre cross-sectional area. MuRF1 and MAFbx gene expression were significantly increased (9- and 3.5-fold, respectively) in the muscle of PC compared to PF rats. Oxygen consumption in non-phosphorylating state and the ATP/O were similar in both groups. Muscle UCP2 gene was overexpressed in PC rats. State III and the uncoupled state were significantly lower in muscle mitochondria from PC rats with a parallel reduction in complex IV activity (−30 %).
Conclusion This study demonstrated that there was neither alteration in ATP synthesis efficiency nor mitochondrial uncoupling in skeletal muscle of cachectic rats despite UCP2 gene overexpression. Muscle mitochondrial oxidative capacities were reduced due to a decrease in complex IV activity. This mitochondrial bioenergetics alteration could participate to insulin resistance, lipid droplet accumulation and lactate production.

Keywords Muscle atrophy · PROb-BDIX model · Energy wasting · Cardiolipin · UCP · COX IV

C. M. Julienne · J.-F. Dumas · C. Goupille · M. Pinault · C. Couet · S. Servais (✉)
INSERM U921, Nutrition, Croissance et Cancer,
37032 Tours, France
e-mail: stephane.servais@univ-tours.fr

C. M. Julienne · J.-F. Dumas · M. Pinault · C. Couet · S. Servais
Université François Rabelais,
37032 Tours, France

C. Goupille · C. Couet
CHRU Bretonneau,
Tours 37044, France

C. Berri · A. Collin · S. Tesseraud
INRA,
UR83 Recherches Avicoles,
37380 Nouzilly, France

S. Servais
IUT,
Tours 37082, France

1 Introduction

Cancer cachexia is a complex syndrome that encompasses a wide range of metabolic, hormonal and cytokine-related abnormalities leading to a negative energy balance due to both anorexia and hypermetabolism resulting in a wasting syndrome. The accelerated breakdown of muscle and adipose tissues providing substrates to the host and the tumour

Published online: 31 May 2012

is responsible for the depletion of lipid and protein stores and account for most of the weight loss [1]. Skeletal muscle atrophy is a major factor involved in cancer cachexia since it contributes to physical disability, weakness and decreased capacity of wound healing and reduces responsiveness to chemotherapy. Skeletal muscle loss in cancer cachexia is due to fibre atrophy, which seems to affect predominantly glycolytic fibres [2, 3]. Research efforts have led to better understanding of the molecular and signalling mechanisms responsible for skeletal muscle atrophy in cancer cachexia. Studies in animals [4] as well as in humans [5] emphasise the ubiquitin–proteasome pathway as the main mechanism for myofibrillar protein degradation. Muscle atrophy F box (MAFbx)/atrogin 1 and muscle RING finger 1 (MuRF1), muscle-specific E3 ligases with function in protein ubiquitination, have been shown to mediate proteosome-dependent protein degradation in cancer cachexia [4, 6]. The ubiquitin–proteasome-dependent proteolysis is an ATP requiring process. Therefore, we can logically wonder how muscle mitochondria deals with these high energy needs for proteolysis in cancer cachexia. The mitochondrial respiratory chain ATP synthesis by the F_1F_0ATP synthase is coupled to oxygen consumption (oxidation). The coupling of the oxidative phosphorylation is modulated in order to maintain energy homeostasis with a compromise between the rate and efficiency of ATP synthesis. During high energy demand, the cost for a high rate of ATP synthesis in mitochondria is a decreased efficiency. These processes represent energy wasting since all oxygen consumed will not be converted into ATP [7, 8]. In this way, we can hypothesise that in a situation of high muscle proteolysis as in cancer cachexia, muscle mitochondria could be the place of energy wasting. If energy wasting (reduction in ATP production efficiency) is occurring in skeletal muscle mitochondria, it could participate significantly to cancer cachexia by increasing energy expenditure since skeletal muscle accounts for 15 to 30 % of the basal energy expenditure [9].

Pioneer indirect evidences for a reduction in oxidative phosphorylation efficiency in skeletal muscle mitochondria in cancer cachexia came from studies reporting uncoupling protein 2 and 3 (UCP) genes overexpression in skeletal muscle in animal model of cancer cachexia [10–15] as well as in patients with cancer [16], or other wasting diseases [17]. Overexpression of UCP2 and UCP3 were considered by these authors as possibly associated to mitochondrial uncoupling, but never experimentally proven. Recently, Constantinou and collaborators [15], using in vivo ^{31}P nuclear magnetic resonance, published interesting data reinforcing the idea that muscle energy production capacities are affected in cancer cachexia. Indeed, skeletal muscle ATP synthesis rate was significantly reduced in mouse model of cancer cachexia. However, to our knowledge, only one study has investigated muscle mitochondrial respiratory chain function in a rat cancer cachexia model [18]. Ushmorov and co-workers found a reduction in oxygen consumption in phosphorylating state (with ATP synthesis) in isolated skeletal muscle mitochondria but data on ATP synthesis efficiency and energy wasting were lacking. Another recent study reported a reduction in cytochrome c oxidase IV (COX IV) protein expression in skeletal muscle of ApcMin/+ cachectic mice [19]. Despite these indirect evidences and arguments, efficiency of skeletal muscle mitochondrial oxidative phosphorylation in cancer cachexia is still unexplored while it can significantly affect energy balance. Therefore, the aim of this study was to determine if efficiency of oxidative phosphorylation is impaired in skeletal muscle mitochondria in a preclinical model of cancer cachexia in rats.

2 Experimental procedures

2.1 Animal care and experimental design

The present investigation received the agreement of the French Ethic Committee 'Region Centre' and was performed in accordance with the French guiding principles in the care and use of animals. Twenty healthy immunocompetent male Berlin–Druckrey IX (BDIX) rats were supplied by Charles River laboratories (L'Arbresle, France) at 8 weeks of age (195±2 g). After arrival, the rats were housed three per cage and were fed ad libitum and weighed weekly.

We used the PROb-BDIX model of cancer cachexia as described previously [20]. At 9 weeks of age, rats were individually housed and acclimated for 2 weeks. During this period, body weight and food intake were measured every 2 days. Then, rats were divided into three groups as follows: (1) one fed ad libitum with tumour inoculation (peritoneal carcinosis, PC; n=10) that received a single IP injection of 10^6 of PROb cells in 1 ml of RPMI 1640 medium [20], (2) one healthy group fed ad libitum that received an IP injection of 1 ml of RPMI 1640 medium without tumour inoculation (Hal; n=10) and (3) one healthy group pair-fed to PC rats (PF, n=10). PF rats, weight-matched to PC rats, received an IP injection of 1 ml of RPMI 1640 medium without tumour inoculation. The use of a pair-fed group as control allowed us to discriminate between the effects of anorexia and hypermetabolism related to cancer cachexia on the parameters measured in this study. The amount of food for the PF rats was based on the food intake measured every 2 days in PC rats until sacrifice (each PC rat was paired with a PF rat).

As we described previously (for details, see [20] and [21]), when PC rats reached severe cachexia state (sacrifice time), food intake was significantly reduced (severe

anorexia, −75±4 % of reduction in comparison to Hal rats). Food intake reduction was progressive during peritoneal carcinosis development and became statistically significant from 24 days after cancer induction (−20 %) until sacrifice (35 days after cancer induction) (−75±4 %).

Body weight (ascites free) of PC rats at sacrifice was significantly lower than in Hal (305±29 vs 378±28 g, respectively) and PF rats (332±21 g) (results published in [20]). Moreover, body weight of PF rats at sacrifice time was significantly lower than in the Hal group [20]. Overall body weight gain was drastically reduced in PC compared to PF rats (0.02 vs 0.1 g/day/100 g of body weight, respectively [20]). At this advanced state of cancer cachexia, TNFα level in serum was higher in PC than in Hal and PF rats (14- and 27-fold. respectively) with a similar level between Hal and PF rats [20].

2.2 Tissue collection

Each PF rat was euthanised 2 days after the paired PC rat, to ensure adequate food restriction period. After blood and ascites collection, muscles were rapidly removed and weighed. The right *quadriceps* was immediately placed in ice-cold isolation medium (sucrose 250 mM, EDTA 1 mM, Tris/HCl 20 mM, pH 7.4) for mitochondrial preparation. Intermediate *vastus* of the other *quadriceps* was frozen in isopentane cooled by liquid nitrogen for later histological analyses. Portions of quadriceps muscle were frozen for RNA and other analyses. All samples were stored at −80°C until analysis.

2.3 *Quadriceps* fibre type and morphometry

Serial cross sections (12 μm thick) of quadriceps muscle were performed at −20°C using a cryostat microtome. All staining procedures were performed according to Remignon et al. [22]. Myofibrillar ATPase activities were assessed after acidic and alkaline pre-incubation at pH 4.35 and 9.40, respectively. Succinate dehydrogenase activity was also evaluated. Fibres were classified as types I, IIa, IIx and IIb according to the classification procedure described by Lind and Kernell [23]. Fibre number by field and fibre cross-sectional area (CSA) were determined on muscle sections stained with azorubin. For each sample, mean CSA was determined on approximately 150 fibres in two random fields. All quantitative analyses were carried out by using a computerised image analysis system (Visilog 4.0, Noesis, Courtaboeuf, France).

2.4 Ubiquitin–proteasome pathway-related protein and UCP2 and UCP3 gene expression

Total RNA was extracted using Trizol according to the manufacturer's recommendations. After RNase-Free DNase treatment, RNA was reverse-transcribed using Super Script II RNase H Reverse Transcriptase (Invitrogen, Carlsbad, CA, USA) and random primers (Promega, Charbonnieres-les-bains, France). Quantitative real-time RT-PCRs were performed in duplicate using an ABI Prism 7000 apparatus (Applied Biosystems, Foster City, CA, USA). The primers chosen for studying the gene expression of two ubiquitin–protein ligases ((E3) MuRF1 and atrogin 1/MAFbx) and UCP2 and UCP3 were specifically designed and validated (Table 1). All primers were obtained from Eurogentec SA (Angers, France). The cycling conditions consisted in a denaturation step (95°C for 10 min) and 35 cycles of amplification, including both denaturation for 15 s at 95°C and annealing–extension for 1 min at 60°C (62°C for UCP2). At the end of the PCR, dissociation was performed by slowly heating the samples from 60 to 95°C and continuous recording of the decrease in SYBR Green fluorescence resulting from the dissociation of double-stranded DNA. Mean PCR efficiency for each target gene was determined by performing five to six serial dilutions of a cDNA pool. The threshold cycle (Ct), defined as the cycle at which an increase in fluorescence above a defined baseline can be first detected, was determined for each sample. The mRNA levels were estimated based on the Ct deviation of an

Table 1 Oligonucleotide primer sequences used for qPCR analysis

Gene	Primers	Product size (bp)	Accession number
MuRF1	Forward: 5′GGT GCC TAC TTG CTC CTT GT3′ Reverse: 5′TCA CCT GGT GGC TGT TTT C3′	203	AY059627.1
MAFbx	Forward: 5′TTA TGC ACG CTG GTC CAG A3′ Reverse: 5′TGT AAG CAC ACA GGC AGG TC3′	170	NM_133521
UCP2	Forward: 5′-ACA AGA CCA TTG CAC GAG AG-3′ Reverse: 5′-CAT GGT CAG GGC ACA GTG GC-3′	293	AF039033
UCP3	Forward: 5′GTG ACC TAT GAC ATC ATC AAG GA3′ Reverse: 5′GCT CCA AAG GCA GAG ACA AAG3′	89	NM_013167
β-Actin	Forward: 5′CTG GCT CCT AGC ACC ATG AA3′ Reverse: 5′CTG CTT GCT GAT CCA CAT CT5′	103	NM_031144

MAFbx Muscle Atrophy F box or Atrogin 1, *MuRF1* Muscle RING Finger 1, *UCP* Uncoupling Protein 2 and 3

unknown sample vs a control cDNA (consisting of a pool of rat muscle cDNA) according to the equation proposed by Pfaffl [24]. Beta-actin was chosen as the reference gene to standardise data.

2.5 Preparation of mitochondria

At sacrifice time, muscle mitochondria were isolated by differential centrifugation as previously described [25]. After mincing, muscle was homogenised using a Potter-Elvenhjem homogeniser (7 strokes) in isolation medium with protease subtilisin A (1 mg/g of muscle). Then, the homogenate was diluted two times and centrifuged at 800× *g* for 10 min. The resulting supernatant was filtered and centrifuged at 10,000× *g* for 10 min. The pellet of muscle mitochondria was resuspended in isolation medium and then centrifuged (10,000× *g*, 10 min). The resulting pellet was resuspended in isolation medium and protein concentration was determined using the bicinchoninic acid assay kit (Interchim) with BSA used as a standard. After protein concentration determination, mitochondrial solution was supplemented with 0.3 % (*w*/*v*) fatty acid-free BSA.

2.6 Mitochondria oxygen consumption

Oxygen was measured using a Clark oxygen electrode (Hansatech, and Rank Brothers Ltd) as previously described [25]. Mitochondria (0.2 mg/ml) were incubated at 37°C in a respiratory reaction medium (KCl 120 mM, KH_2PO_4 5 mM, EGTA 1 mM, $MgCl_2$ 2 mM, Hepes 3 mM, pH 7.4) saturated with ambient air. Oxygen consumption rate was measured with succinate (5 mM) as substrate in the presence of rotenone (2.5 μM, complex I inhibitor). Next, oxygen consumption in phosphorylating state (state III) was initiated by the addition of ADP (300 μM). Then, oligomycin (2 μg/mg of protein, inhibitor of ATP synthase) was added to measure non-phosphorylating oxygen consumption rate (state IV). Afterwards, the uncoupled state of oxygen consumption was initiated by the addition of carbonyl cyanide p-trifluoromethoxyphenylhydrazone (FCCP, 2 μM). The respiratory control ratio (RCR) refers to the ratio state III/state IV. The integrity of isolated mitochondria was checked by the addition of exogenous cytochrome c. A significant increase in oxygen consumption after cytochrome c is an index of damaged mitochondria.

2.7 Mitochondrial ATP synthesis

The rate of ATP synthesis was followed by glucose 6-phosphate accumulation using an ADP regenerating system based on hexokinase plus glucose and ATP as previously described [21]. The respiratory reaction medium as described above was supplemented with 5 mM succinate, 5 μM rotenone, 20 mM glucose and 125 μM ATP. ATP synthesis was modulated by a sequential increase in hexokinase concentration at 37°C. Glucose 6-phosphate formation was monitored from NADPH content by spectrophotometry at 340 nm.

2.8 Determination of cytochrome c oxidase protein expression by western blotting

Equal amounts of *quadriceps* mitochondrial proteins (5 μg) were boiled in the loading buffer and resolved by 12.5 % SDS polyacrylamide gels. For immunoblotting, proteins were transferred onto a polyvinylidene difluoride membrane (Immobilon-P Transfer Membrane; Millipore) with 3-(cyclohexylamino)-1-propane sulfonic acid electroblotting buffer for 2 h at 150 mA. The blot was blocked overnight in a blocking buffer (5 % non-fat milk in phosphate-buffered saline solution, PBS), washed three times in PBS–Tween 20 for 5 min and probed for 2 h at room temperature with a monoclonal antibody anti-complex IV (1:20,000; Mitosciences). The blot was washed three times for 5 min in PBS–Tween 20 and probed for 1 h at room temperature with peroxidase-conjugated goat anti-mouse IgG (1:3,000; SouthernBiotech). Signals were visualised on high-performance chemiluminescence film (Sigma) using an enhanced chemiluminescence procedure (Amersham France). The membranes were scanned and the signals were analysed with Quantity One software (Bio-Rad).

2.9 Cytochrome c oxidase activity

COX activity was measured by spectrophotometry in isolated *quadriceps* mitochondria (10 μg of protein) as previously described [26].

2.10 Cardiolipin content

Cardiolipins were quantified by incubating (10 min, 37°C) 0.2 mg mitochondrial protein in 2 ml of isolation medium containing increasing concentrations of 10-N-nonyl acridine orange (NAO; 80–150 μM) [21]. Then, samples were centrifuged at 10,000× *g* for 10 min and unbound NAO was measured in supernatants with a fluorescence spectrophotometer (Hitachi) (excitation–emission 496–530 nm). The amount of dyes bound was calculated by subtracting the amount found in the supernatant from the total added amount.

2.11 Statistical analysis

Data are presented as mean ± standard error of the mean (SEM). Statistical analyses were performed by

using Graph Pad Prism®. Differences between groups were analysed by non-parametric Mann–Whitney test. Correlations were analysed by Spearman non-parametric test. Differences of $p<0.05$ were considered significant.

3 Results

3.1 Peritoneal carcinosis induces muscle wasting

Muscle loss was evaluated on main hindlimb muscles, with various compositions in fibre type, as *quadriceps* (Quad), *extensor digitorum longus* (EDL), *gastrocnemius* (Gast), *plantaris* (PL), *soleus* (Sol) and *tibialis anterior* (TA). There was no effect of calorie restriction per se (PF rats *vs* Hal rats) on the six muscle weights (Table 2). All muscles but slow oxidative *soleus* had a significant weight reduction (from 7 to 10 %) in PC rats compared to PF rats (Table 2).

3.2 Muscle loss is due to fibre atrophy and is related to an up-regulation of ubiquitin–proteasome-related genes

Gene expression of MuRF1 and MAFbx in *quadriceps* was largely significantly increased in PC rats compared to PF and Hal rats (Fig. 1). Analysis of fibre type composition and CSA in quadriceps muscle demonstrated a significant reduction in fibre CSA in PC rats in comparison to PF rats (Fig. 2). PC rats had a significant increase in proportion of fibres with CSA of 500 to 1,000 μm and 1,000 to 1,500 μm (6- and 2-fold increase, respectively) in comparison to PF rats. In contrast, the percentage of larger fibres (>5,500 μm) was lower in PC rats than in PF rats (5,500 to 6,000 μm—3-fold with $p<0.05$ and >6,000 μm—4-fold with $p=0.055$) (Fig. 2a). Compared to PF rats, the mean CSA area of type IIa/IIx and IIb fibres in the quadriceps of PC rats was significantly reduced (−27 and −33 %, respectively; Fig. 2b).

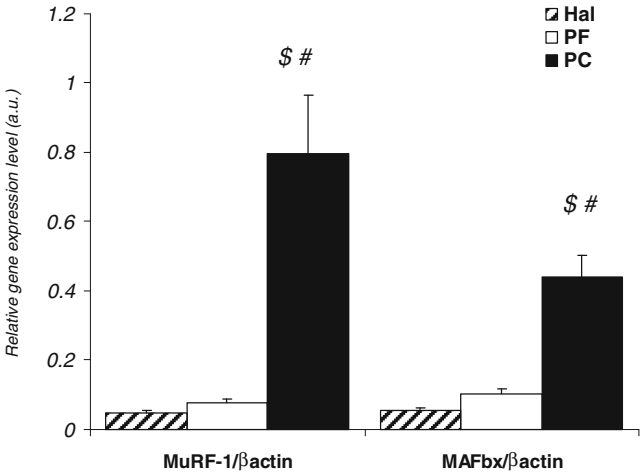

Fig. 1 Proteolysis in *quadriceps* muscle from peritoneal carcinosis (PC), pair-fed (PF) and healthy ad libitum (Hal) rats. MuRF1 and MAFbx gene expression, with PF ($n=10$) and PC ($n=10$). Gene expression levels were normalised for β-actin mRNA. Values are means ± SEM. Statistical significance was set at $p<0.05$. *Number sign*, significantly different from PF. *Dollar sign*, significantly different from Hal

3.3 Evidences for muscle mitochondria bioenergetics alterations in cachectic rats

The linear relationship between ATP synthesis rate and oxygen consumption (ATP/O) was similar between PC and PF rats (Fig. 3) since the intercept and slope of the two regression lines were not different. However, the oxygen consumption at the highest hexokinase concentration (highest ATP synthesis rate) was significantly lower in PC compared to PF (649±36 and 846±36

Table 2 Hindlimb muscles weight in healthy ad libitum (Hal), pair-fed (PF) and peritoneal carcinosis (PC) rats expressed in milligram of muscle and in milligram per 100 g of body weight (BW)

	Quad	EDL	TA	Sol	PL	Gast
Hal (mg)	5,692±265	398±38	1,261±43	259±28	559±94	3,149±333
PF (mg)	5,131±561	367±25	1,233±64	248±14	500±39	2,888±164
PC (mg)	4,226±409[a,b]	309±59[a,b]	976±101[a,b]	224±32[a,b]	418±28[a,b]	2,471±174[a,b]
Hal (mg/100 g of BW)	1,538±91	108±13	341±20	70±8	153±24	867±115
PF (mg/100 g of BW)	1,544±94	111±6	372±15	75±5	151±12	874±68
PC (mg/100 g of BW)	1,388±76[a,b]	103±27[b]	322±36[b]	73±6	138±11[b]	814±55[b]

Values are the mean of the left and right muscle weights. With Hal ($n=10$), PF ($n=10$) and PC ($n=10$). Values are means ± SEM. Statistical significance was set at $p<0.05$

Quad *quadriceps*, EDL *extensor digitorum longus*, TA *tibialis anterior*, Sol *soleus*, PL *plantaris*, Gast *gastronemius*

[a] Significantly different from Hal

[b] Significantly different from PF

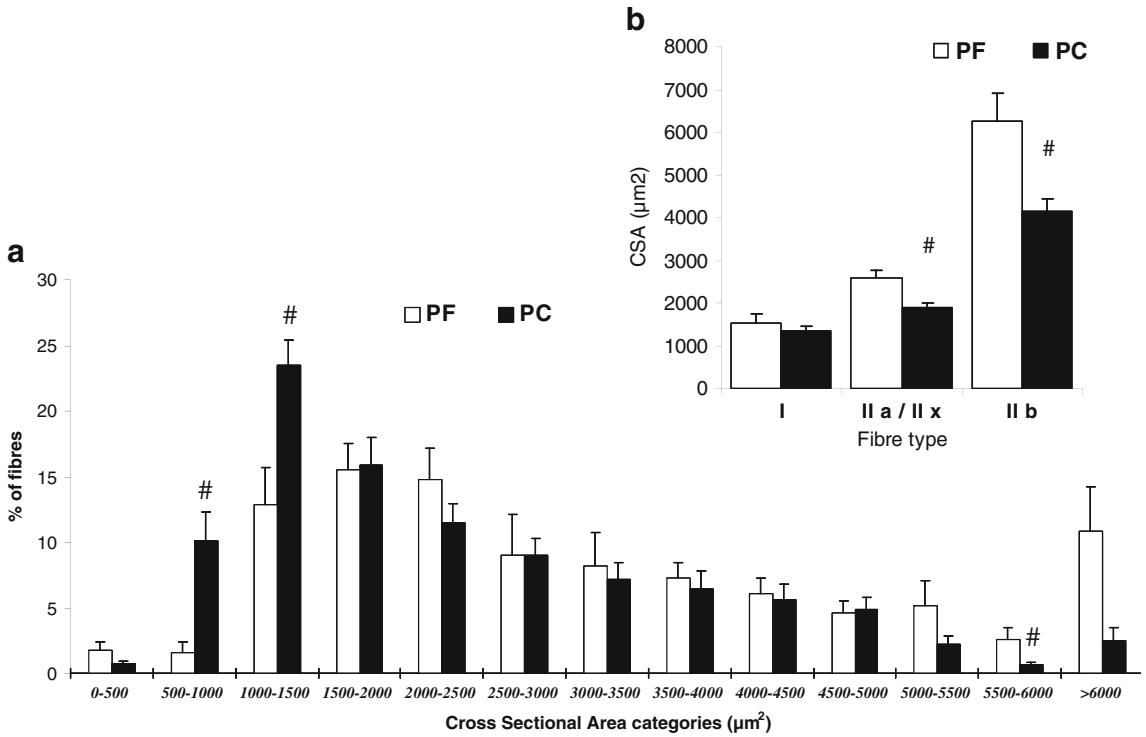

Fig. 2 Distribution of *quadriceps* fibres according to cross-sectional area (CSA) and mean cross-sectional area of type I, IIa/IIx and IIb fibres in pair-fed (PF) and peritoneal carcinosis (PC) rats. **a** Distribution of *quadriceps* fibres and **b** mean cross-sectional area. CSA were determined on approximately 150 fibres in two random fields in PF rats (n=4) and PC rats (n=7). Values are means ± SEM. Statistical significance was set at $p<0.05$. *Number sign*, significantly different from PF

natoms/min per mg protein, respectively, p=0.004). In the same way, at the highest oxygen consumption common to PC and PF rats of the ATP to oxygen consumption relationship, ATP synthesis rate was reduced by 20 % in PC rats compared to PF rats, without reaching statistically significant difference.

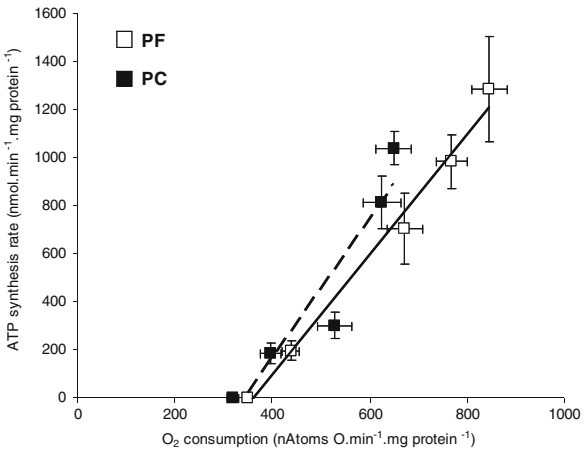

Fig. 3 Efficiency of ATP synthesis in isolated quadriceps mitochondria from pair-fed (PF) and peritoneal carcinosis (PC) rats. ATP/O: relationship between oxygen consumption and ATP synthesis rate. With PF (n=10) and PC (n=10), ATP synthesis was measured by the addition of increasing hexokinase concentration. Values are means ± SEM

Oxygen consumption of *quadriceps* mitochondria in phosphorylating state (state III) and uncoupled state (with FCCP) was significantly reduced (−20 and −16 %, respectively) in PC rats compared to PF rats (Table 3). These differences between PC and PF rats were not due to damages induced by mitochondrial isolation procedure. In fact, cytochrome c stimulation of oxygen consumption (in percent) was low and similar in both groups (PC—8.8±3.5 and PF—7.0±3.4). The oxygen consumption in non-phosphorylating state (state IV, with oligomycin) in PC rats was not different from PF rats. Respiratory control ratio (state III to state IV ratio) of skeletal muscle mitochondria was not affected by peritoneal carcinosis-induced cachexia (Table 3). *Quadriceps* UCP2 gene expression was 3.7 times higher in PC rats compared to PF rats. However, UCP3 gene expression was similar between both groups (Fig. 4).

3.4 Reduction in muscle mitochondrial oxidative capacities is due to reduction in cytochrome c oxidase activity

Cytochrome c oxidase (complex IV) expression was similar in PC and PF rats (Fig. 5a, b). The activity of complex IV was significantly reduced by 30 % in PC rats compared to PF rats (Fig. 5c). There was a positive significant correlation (R^2=0.74, p=0.033) between complex IV activity and

Table 3 Mitochondrial oxygen consumption in *quadriceps* of pair-fed (PF, $n=10$) and peritoneal carcinosis (PC, $n=10$) rats

In natoms/min/mg of proteins	State III	State IV	Uncoupled state	RCR
PF	600±20	137±4	603±18	4.4±0.2
PC	480±20[a]	124±5	508±25[a]	3.9±0.2

The measurements were run with succinate as energy substrate. State III: phosphorylating state was performed in the presence of ADP; state IV: non-phosphorylating state was obtained after the addition of oligomycin; uncoupled state was determined with the uncoupling reagent FCCP. The RCR was calculated as state III/state IV. Values are means ± SEM. Statistical significance was set at $p<0.05$

[a] Significantly different from PF

maximal oxygen consumption (uncoupled state) (Fig. 6). This correlation was the same when complex IV activity was determined by oxygraphy (with TMPD ascorbate as substrate, R^2 0.8, $p=0.01$, data not shown).

3.5 Lower oxidative capacities are not associated to cardiolipin content modification

Cardiolipin content in quadriceps mitochondria was similar in PC and PF rats (respectively, 177±9 vs 182±10 nmol/mg protein).

4 Discussion

Cancer cachexia is the consequence of a negative energy balance due to both anorexia and hypermetabolism, resulting in a wasting syndrome. Skeletal muscle atrophy is a main target of cancer cachexia. Direct and indirect evidences suggested the implication of mitochondrial bioenergetics disorders in muscle loss during cancer cachexia. Hypotheses about these bioenergetics disorders are mitochondrial uncoupling and/or alteration of ATP synthesis rate. Therefore, the aim of this study was to determine if efficiency of oxidative phosphorylation is impaired in skeletal muscle mitochondria in a preclinical model of cancer cachexia in rats.

We had previously validated the model of cancer induced by peritoneal carcinosis in BDIX rats [20]. It is a useful preclinical model in cancer cachexia field because peritoneal carcinosis is a serious clinical situation with a poor prognosis that is frequent in several cancer types, such as ovarian, pancreatic, stomach or colorectal cancers. We have demonstrated the occurrence of hallmarks of the syndrome:

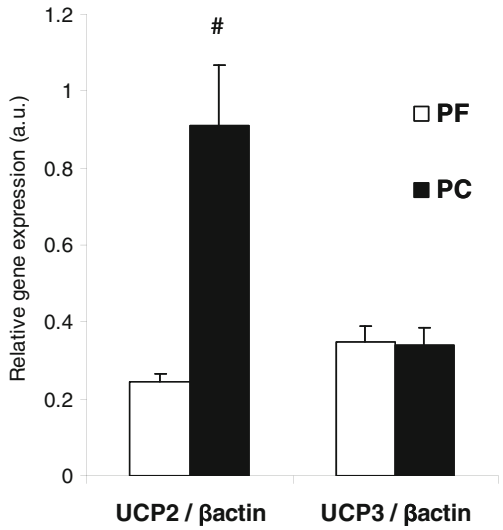

Fig. 4 UCP2 and UCP3 gene expression in isolated *quadriceps* mitochondria from pair-fed (PF) and peritoneal carcinosis (PC) rats. With PF ($n=8$) and PC ($n=8$). Values are means ± SEM. Statistical significance was set at $p<0.05$. *Number sign*, significantly different from PF

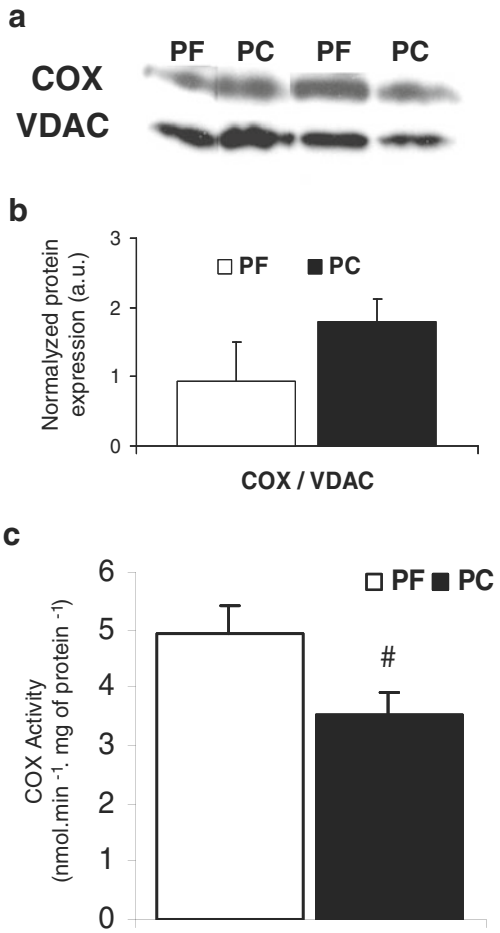

Fig. 5 Cytochrome c oxidase (COX) protein expression and activity in isolated *quadriceps* mitochondria from pair-fed (PF) and peritoneal carcinosis (PC) rats. **a** Western blots of COX protein expression, **b** Quantification using Quantity One software (Bio-Rad) of the ratio COX/VDAC protein expression. With PF ($n=6$) and PC ($n=6$), **c** Enzymatic activity of COX. With PF ($n=4$) and PC ($n=4$). Values are means ± SEM. Statistical significance was set at $p<0.05$. *Number sign*, significantly different from PF

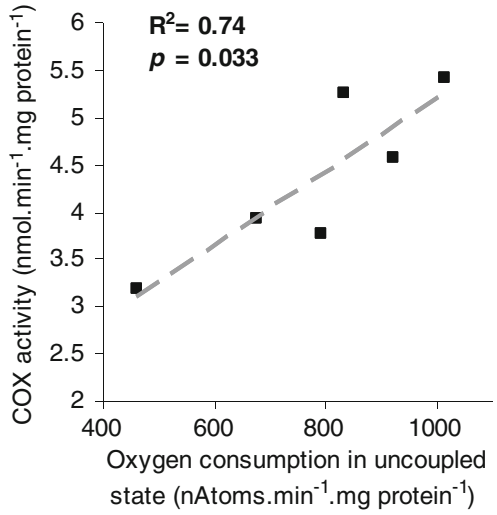

Fig. 6 Relationship between cytochrome c oxidase activity and maximal oxygen consumption in uncoupled state in *quadriceps* isolated mitochondria. The correlation was tested by non-parametric Spearman test

anorexia, systemic inflammation, white adipose and skeletal muscle wasting. Furthermore, the use of pair-fed rats demonstrated the presence of a hypermetabolism [20]. The first step of the present study was to check if the model of peritoneal carcinosis-induced cachexia in BDIX rats was presenting the main specific characteristics of muscle wasting described in animal and human studies. Focussing on main hindlimb muscles as *quadriceps* (Quad), *extensor digitorum longus* (EDL), *gastrocnemius* (Gast), *plantaris* (PL), *soleus* (Sol) and *tibialis anterior* (TA) that presented various compositions in fibre type, we found that the *soleus* was the only muscle unaffected by peritoneal carcinosis. These results are in agreement with previous studies reporting that fast glycolytic muscles are more susceptible to wasting in cancer cachexia [27]. Muscle wasting in the present study was associated to a large increase in the expression of two major genes involved in the ubiquitin–proteasome system, MuRF1 and MAFbx, in *quadriceps* PC rats in comparison to Hal and PF rats as reported by numerous studies [4, 6].

Since there was no difference between Hal and PF rats in muscle weight and proteolysis-related gene expression, we chose to use PF rats as control for PC rats for the analysis of the following data. Moreover, the aim of the present study was to investigate if energy wasting (reduction in ATP production efficiency) was occurring in skeletal muscle mitochondria keeping in mind that it could contribute to cancer cachexia-related hypermetabolism. In this way, the pair-fed group allowed us to discriminate between the effects of anorexia and hypermetabolism related to cancer cachexia on the parameters measured in this study.

Muscle morphology study indicates that muscle loss observed in rat with peritoneal carcinosis was due to a reduction in fibre CSA rather that in its number. From these data, we can conclude that peritoneal carcinosis induction in BDIX rats reached all characteristics of cancer cachexia, since in addition to what we described previously [20], there was a clear muscle atrophy affecting fast-twitch fibres associated to large up-regulation of the ubiquitin–proteasome pathway. Thus, the PROb-BDIX model is a suitable model to investigate mechanisms involved in cancer cachexia and specifically to study mitochondrial bioenergetics in *quadriceps* muscle wasting.

In order to elucidate if there are alterations in energy production yield in skeletal muscle mitochondria in cancer cachexia, we performed a complete analysis of mitochondrial bioenergetics. Our study is the first investigating the efficiency of oxidative phosphorylation, in isolated skeletal muscle mitochondria in a preclinical cancer cachexia model. The ATP synthesis efficiency was sought by measuring the relationship between oxygen consumption and ATP synthesis rate (ATP/O). The ATP/O was similar between PC and PF rats. Therefore, we clearly demonstrated that ATP synthesis efficiency was unchanged in *quadriceps* mitochondria in our rat model of cancer cachexia (Fig. 3).

The absence of alteration in oxidative phosphorylation efficiency in PC rats compared to PF rats is contradictory with the previously suggested mitochondrial uncoupling (by UCPs) reported in skeletal muscle [10–12, 14–16]. In our study, the absence of mitochondrial uncoupling was confirmed by similar oxygen consumption in non-phosphorylating state (state IV) in PC rats and PF rats. In fact, state IV is described as the oxygen consumption necessary to compensate loss of electrochemical gradient, considered as uncoupling due to proton leak. Moreover, respiratory control ratio (state III/state IV) of skeletal muscle mitochondria was not affected by peritoneal carcinosis-induced cachexia. The absence of uncoupling was concomitant with overexpression of UCP2 gene in skeletal muscle in PC rats compared to PF. Surprisingly, there was no difference in UCP3 expression. These later data need to be compared with the study that had designed pair-fed groups as calorie restriction is well known to increase UCP2 and UCP3 expression [28, 29]. Since PF rats had a significant increase of 74 % in UCP3 gene expression in comparison to Hal rats (data not shown), our study is in agreement with studies reporting that UCP3 gene expression is related to calorie intake [10, 11]. As mitochondrial uncoupling is unlikely, our data clearly questioned the role of UCP2 in skeletal muscle during cancer cachexia. The physiological and pathological roles of UCP2 and UCP3 are still a large subject of debate [30]. However, we can highlight the suggested function of UCP2 as antioxidant defence by reducing mitochondrial reactive oxygen species production (ROS)

[31, 32]. To reinforce this potential antioxidant role of UCP2, we have shown that there was no difference in *quadriceps* mitochondrial ROS production in PC and PF rats (data not shown).

Even though the global analysis (slope and intercept) of ATP/O indicates no alteration in ATP synthesis efficiency, some difference come to light. In this way, the oxygen consumption at the highest hexokinase concentration (highest ATP synthesis rate) was significantly lower in PC compared to PF (Fig. 3). In the same way, at the highest oxygen consumption common to PC and PF rats of ATP/O, ATP synthesis rate was reduced by 20 % in PC rats compared to PF rats, without reaching statistically significant difference. Our data are in agreement with the significant reduction in skeletal muscle ATP synthesis rate, measured in vivo by ^{31}P NMR, in mice implanted with Lewis lung carcinoma [15]. This suggests that the reduction in the rate of ATP synthesis observed in vivo is rather due to a reduction in the respiratory chain activity than an alteration of the ATP synthesis efficiency.

We confirmed the reduction in respiratory chain activity by performing oxygraphic measurement on isolated mitochondria. In fact, *quadriceps* mitochondrial oxygen consumption in the phosphorylating state and in the uncoupled state was significantly reduced in PC rats compared to PF rats. These data clearly demonstrate lower muscle mitochondrial oxidative capacities in PC rats compared to PF suggesting alterations in content and/or activity of respiratory chain complexes. Because complex IV is one of the main regulator of oxidative phosphorylations in skeletal muscle [33], we measured the activity and protein content of this respiratory complex. While complex IV expression was unaffected by cancer cachexia, activity was significantly decrease in PC compared to PF rats. Such dysfunctions were reported by Ushmorov and collaborators [18] with C57BL/6 mice bearing fibrosarcoma MCA-105 as model of cancer cachexia. These authors demonstrated that in the phosphorylating state, skeletal muscle mitochondria from tumour-bearing mice displayed significant reduction in oxygen consumption at complexes II–III and IV in comparison to control mice. More specifically, as the protocol was set by Ushmorov and co-workers, the measurement of 'complexes II–III' activities was in fact 'complex II–III–IV' activities since complex IV is the final electron acceptor of the respiratory chain. Thus, by reporting around the same percent of reduction (−20 and −25 %) in the activities of complexes 'II–III–IV' and IV alone, these authors provided evidence for an alteration in complex IV activity in skeletal muscle-isolated mitochondria from cachectic animals in complete accordance with our data. We confirmed the specific implication of complex IV in oxidative capacities reduction with a positive significant correlation between COX activity and uncoupled state oxygen consumption (Fig. 6).

Among the regulators of complex IV activity, cardiolipins, a specific phospholipid class of mitochondrial membranes, have been clearly identified [34]. In the present study, the cardiolipin content in *quadriceps* mitochondria was not affected by cancer cachexia. As oxidative stress was clearly associated to muscle wasting [3], we cannot exclude the occurrence of cardiolipin peroxidation that was reported to affect COX activity [35]. Direct oxidative damages of complex IV by lipid-derived protein adducts (4-HNE and MDA) cannot be ruled out since protein oxidative damages were reported in *gastrocnemius* muscle in AH-130 Yoshida hepatoma rat model [3]. However, these authors found ATP synthase as the only oxidative phosphorylation-related protein affected by lipid peroxidation by-products. Lastly, because COX activity is known to be regulated by ATP [36], we can hypothesise that reduction in COX is due to a higher allosteric ATP inhibition by modulation of COX phosphorylation.

A reduced mitochondrial oxidative capacity in muscle during cancer cachexia is somehow paradoxical since proteolysis by the ubiquitin–proteasome system is ATP dependent. In this condition, additional ATP supply is produced by anaerobic glycolytic energy pathways with lactate production. Thus, skeletal muscle mitochondrial alterations could participate significantly to the increase in plasma lactate concentration supplying the futile Cori cycle that participate to the increase in whole body energy needs. Moreover, we can speculate that reduction in skeletal muscle oxidative capacities could play a significant role in (1) lipid droplet accumulation [37] and (2) insulin resistance [38] that are occurring during cancer cachexia [1].

5 Conclusion

The PROb-BDIX rat model is suitable to investigate the mechanisms involved in cancer cachexia and specifically in muscle wasting and the potential implication of mitochondrial bioenergetics alterations. Moreover, this model can be used to test nutritional and pharmacological strategies to limit muscle atrophy in cancer cachexia. First, our study confirms that skeletal muscle mitochondrial bioenergetics alterations are present in cancer cachexia. The nature of these alterations is not related to energy wasting but to a reduction in mitochondrial oxidative capacities due to a decrease in complex IV activity. This could be responsible for a reduction in ATP production in muscle mitochondria without modification of ATP synthesis efficiency. The present study brings new pieces in the puzzle of mitochondrial implication in muscle wasting. The mechanisms implicated in the reduction in muscle mitochondrial complex IV activity in cachectic rat need to be fully explored.

Acknowledgments This work was supported by Ligue Contre le Cancer (comités 37 and 28), Conseil Régional de la Région Centre and Canceropole Grand Ouest (axe Valorisation des produits de la mer en cancérologie)'. Julienne C.M. PhD was supported by 'Conseil Régional de la Région Centre'. Dumas J.F. was supported by a grant from 'Conseil Régional de la Région Centre' and 'Société Francophone Nutrition Clinique et Métabolisme' (SFNEP). Goupille C. was supported by CHRU Bretonneau Tours. The authors thank Sabine Crochet and Thierry Bordeau (INRA, UR83 Recherches Avicoles, F-37380 Nouzilly) for their skilled technical assistance, and Valérie Schnubel, George Roseau, Jérome Montharu and Michele Demonte for their help in animal care at the animal facility (College of Medicine). The authors of this manuscript certify that they complied with the ethical guidelines for authorship and publishing in the *Journal of Cachexia, Sarcopenia and Muscle* [39].

Conflict of interest The authors declare that they have no conflict of interest.

References

1. Tisdale MJ. Mechanisms of cancer cachexia. Physiol Rev. 2009;89:381–410.
2. Acharyya S, Butchbach ME, Sahenk Z, Wang H, Saji M, Carathers M, et al. Dystrophin glycoprotein complex dysfunction: a regulatory link between muscular dystrophy and cancer cachexia. Cancer Cell. 2005;8:421–32.
3. Marin-Corral J, Fontes CC, Pascual-Guardia S, Sanchez F, Olivan M, Argiles JM, et al. Redox balance and carbonylated proteins in limb and heart muscles of cachectic rats. Antioxid Redox Signal. 2010;12:365–80.
4. Argiles JM, Lopez-Soriano FJ, Busquets S. Mechanisms to explain wasting of muscle and fat in cancer cachexia. Curr Opin Support Palliat Care. 2007;1:293–8.
5. Khal J, Hine AV, Fearon KC, Dejong CH, Tisdale MJ. Increased expression of proteasome subunits in skeletal muscle of cancer patients with weight loss. Int J Biochem Cell Biol. 2005;37:2196–206.
6. Attaix D, Combaret L, Bechet D, Taillandier D. Role of the ubiquitin–proteasome pathway in muscle atrophy in cachexia. Curr Opin Support Palliat Care. 2008;2:262–6.
7. Nogueira V, Rigoulet M, Piquet MA, Devin A, Fontaine E, Leverve XM. Mitochondrial respiratory chain adjustment to cellular energy demand. J Biol Chem. 2001;276:46104–10.
8. Leverve XM. Mitochondrial function and substrate availability. Crit Care Med. 2007;35:S454–60.
9. Rolfe DF, Brown GC. Cellular energy utilization and molecular origin of standard metabolic rate in mammals. Physiol Rev. 1997;77:731–58.
10. Sanchis D, Busquets S, Alvarez B, Ricquier D, Lopez-Soriano FJ, Argiles JM. Skeletal muscle UCP2 and UCP3 gene expression in a rat cancer cachexia model. FEBS Lett. 1998;436:415–8.
11. Bing C, Brown M, King P, Collins P, Tisdale MJ, Williams G. Increased gene expression of brown fat uncoupling protein (UCP)1 and skeletal muscle UCP2 and UCP3 in MAC16-induced cancer cachexia. Cancer Res. 2000;60:2405–10.
12. Busquets S, Carbo N, Almendro V, Figueras M, Lopez-Soriano FJ, Argiles JM. Hyperlipemia: a role in regulating UCP3 gene expression in skeletal muscle during cancer cachexia? FEBS Lett. 2001;505:255–8.
13. Bing C, Russell ST, Beckett EE, Collins P, Taylor S, Barraclough R, et al. Expression of uncoupling proteins-1, -2 and -3 mRNA is induced by an adenocarcinoma-derived lipid-mobilizing factor. Br J Cancer. 2002;86:612–8.
14. Busquets S, Almendro V, Barreiro E, Figueras M, Argiles JM, Lopez-Soriano FJ. Activation of UCPs gene expression in skeletal muscle can be independent on both circulating fatty acids and food intake. Involvement of ROS in a model of mouse cancer cachexia. FEBS Lett. 2005;579:717–22.
15. Constantinou C, Fontes de Oliveira CC, Mintzopoulos D, Busquets S, He J, Kesarwani M, et al. Nuclear magnetic resonance in conjunction with functional genomics suggests mitochondrial dysfunction in a murine model of cancer cachexia. Int J Mol Med. 2011;27:15–24.
16. Collins P, Bing C, McCulloch P, Williams G. Muscle UCP-3 mRNA levels are elevated in weight loss associated with gastrointestinal adenocarcinoma in humans. Br J Cancer. 2002;86:372–5.
17. Tzika AA, Mintzopoulos D, Mindrinos M, Zhang J, Rahme LG, Tompkins RG. Microarray analysis suggests that burn injury results in mitochondrial dysfunction in human skeletal muscle. Int J Mol Med. 2009;24:387–92.
18. Ushmorov A, Hack V, Droge W. Differential reconstitution of mitochondrial respiratory chain activity and plasma redox state by cysteine and ornithine in a model of cancer cachexia. Cancer Res. 1999;59:3527–34.
19. White JP, Baltgalvis KA, Puppa MJ, Sato S, Baynes JW, Carson JA. Muscle oxidative capacity during IL-6-dependent cancer cachexia. Am J Physiol Regul Integr Comp Physiol. 2011;300:R201–11.
20. Dumas JF, Goupille C, Pinault M, Fandeur L, Bougnoux P, Servais S, et al. n-3 PUFA-enriched diet delays the occurrence of cancer cachexia in rat with peritoneal carcinosis. Nutr Cancer. 2010;62:343–50.
21. Dumas JF, Goupille C, Julienne CM, Pinault M, Chevalier S, Bougnoux P, et al. Efficiency of oxidative phosphorylation in liver mitochondria is decreased in a rat model of peritoneal carcinosis. J Hepatol. 2011;54:320–7.
22. Remignon H, Gardahaut MF, Marche G, Ricard FH. Selection for rapid growth increases the number and the size of muscle fibres without changing their typing in chickens. J Muscle Res Cell Motil. 1995;16:95–102.
23. Lind A, Kernell D. Myofibrillar ATPase histochemistry of rat skeletal muscles: a "two-dimensional" quantitative approach. J Histochem Cytochem. 1991;39:589–97.
24. Pfaffl MW. A new mathematical model for relative quantification in real-time RT-PCR. Nucleic Acids Res. 2001;29:e45.
25. Servais S, Couturier K, Koubi H, Rouanet JL, Desplanches D, Sornay-Mayet MH, et al. Effect of voluntary exercise on H_2O_2 release by subsarcolemmal and intermyofibrillar mitochondria. Free Radic Biol Med. 2003;35:24–32.
26. Dumas JF, Roussel D, Simard G, Douay O, Foussard F, Malthiery Y, et al. Food restriction affects energy metabolism in rat liver mitochondria. Biochim Biophys Acta. 2004;1670:126–31.
27. Acharyya S, Guttridge DC. Cancer cachexia signaling pathways continue to emerge yet much still points to the proteasome. Clin Cancer Res. 2007;13:1356–61.
28. Asami DK, McDonald RB, Hagopian K, Horwitz BA, Warman D, Hsiao A, et al. Effect of aging, caloric restriction, and uncoupling protein 3 (UCP3) on mitochondrial proton leak in mice. Exp Gerontol. 2008;43:1069–76.
29. Bevilacqua L, Ramsey JJ, Hagopian K, Weindruch R, Harper ME. Long-term caloric restriction increases UCP3 content but decreases proton leak and reactive oxygen species production in rat skeletal muscle mitochondria. Am J Physiol Endocrinol Metab. 2005;289:E429–38.

30. Cioffi F, Senese R, de Lange P, Goglia F, Lanni A, Lombardi A. Uncoupling proteins: a complex journey to function discovery. Biofactors. 2009;35:417–28.
31. Arsenijevic D, Onuma H, Pecqueur C, Raimbault S, Manning BS, Miroux B, et al. Disruption of the uncoupling protein-2 gene in mice reveals a role in immunity and reactive oxygen species production. Nat Genet. 2000;26:435–9.
32. Mailloux RJ, Harper ME. Uncoupling proteins and the control of mitochondrial reactive oxygen species production. Free Radic Biol Med. 2011;51:1106–15.
33. Rossignol R, Letellier T, Malgat M, Rocher C, Mazat JP. Tissue variation in the control of oxidative phosphorylation: implication for mitochondrial diseases. Biochem J. 2000; 347:45–53.
34. Schlame M, Ren M. The role of cardiolipin in the structural organization of mitochondrial membranes. Biochim Biophys Acta. 2009;1788:2080–3.
35. Musatov A. Contribution of peroxidized cardiolipin to inactivation of bovine heart cytochrome c oxidase. Free Radic Biol Med. 2006;41:238–46.
36. Kadenbach B, Ramzan R, Wen L, Vogt S. New extension of the Mitchell theory for oxidative phosphorylation in mitochondria of living organisms. Biochim Biophys Acta. 2010;1800:205–12.
37. Stephens NA, Skipworth RJ, Macdonald AJ, Greig CA, Ross JA, Fearon KC. Intramyocellular lipid droplets increase with progression of cachexia in cancer patients. J Cachexia Sarcopenia Muscle. 2011;2:111–7.
38. Dumas JF, Simard G, Flamment M, Ducluzeau PH, Ritz P. Is skeletal muscle mitochondrial dysfunction a cause or an indirect consequence of insulin resistance in humans? Diabetes Metab. 2009;35:159–67.
39. von Haehling S, Morley JE, Coats AJ, Anker SD. Ethical guidelines for authorship and publishing in the *Journal of Cachexia, Sarcopenia and Muscle*. J Cachexia Sarcopenia Muscle. 1:7–8.